GATECH Computational Journal: Image Reconstruction Using the Filtered Back-projection and Iterative Method

Jackson L. Browne[a*]
[a]Georgia Institute of Technology, Computational Physics, School of Physics, 837 State St NW, Atlanta, Georgia, 30332

Abstract. The term "computed tomography," or CT refers to a digital x-ray imaging procedure in which a narrow beam of x-rays scans across a patient in synchrony with a radiation detector on the opposite side of the patient. If a sufficient number of transmission measurements are taken at different orientations of the x-ray source and detector, the distribution of attenuation coefficients within the layer may be determined. There are numerous computational algorithms used to reconstruct CT images, however this report will focus on only two. Reconstruction of the image can be done either using the filtered back projection method or iterative reconstruction method. Here we show the efficacy of the two reconstruction algorithms and highlight the differences between them. Despite not being able to quantitatively describe the difference between the reconstructed image and the original the filtered back-projection algorithm produced an image that stands up to par. The iterative reconstruction method was able to produce the exact image using a linear equation solver. However, there are conditions regarding the number of equations needed to produce a correct solution. Iterative reconstruction algorithms are slowly taking the place of filtered back-projection due to their speed and reduction of radiation dose to patients. Nevertheless, each technique has its pros and cons and it is up to the clinical staff to decide which in most appropriate/effective for both the patient and workflow.

*Jackson L. Browne, jbrowne31@gatech.edu, https://github.com/JacksonLBrowne/Final-Report.git

1 Introduction

Image reconstruction is an increasingly complex field in CT. Iterative reconstruction and filtered back-projection (FBP) reconstruction are competing algorithms, however iterative reconstruction could soon replace FBP, mainly, due to its potential for scanning at low radiation doses. The future of CT will inevitably involve shorter scan time and reduced radiation dose, thus evermore following the "As Low As Reasonably Achievable (ALARA)," principle [2]. FBP is computationally efficient, but the filtering step enhances the noise in the CT image. By virtue of the iterative nature of reconstruction, IR images are less noisy than FBP images.

Filtered back-projection is the most commonly used reconstruction method, first introduced by Bracewell and Riddle for astronomy and rediscovered for electron tomography by Ramachadran and Lakshminarayanan [1]. The analytical algorithm itself is designed to overcome the limitations of conventional back projection; it applies a convolution filter to remove blurring [2]. It utilizes simultaneous equations of x-ray sums taken at differing angles to compute the values of attenuation coefficients within a CT slice (cross section). The attenuated profile or projection produced represented by the anatomy is stored in the memory of the computer, solved and reconstructed [2]. Each pixel corresponds to the voxel of the image.

Iterative reconstruction refers to the reconstruction of an CT image beginning with a *guess* made about the image, or it could be a constant or filtered back-projection image. The iteration process then goes through a series of updates (iterations), which drive the CT image toward a final accurate depiction of the object that was scanned. It is recognized that iterative algorithms can model many of the physical parameters that filtered back-projection cannot, such as x-ray spectrum, the blurring of the focal spot etc., and therefore in principle, iterative algorithms can make better use of the acquired data [3].

2 Physics

2.1 Simple Back-projection

When an X-ray beam passes through through a patient, the intensity of the beam decreases exponentially with distance traveled due to the x-ray photons interacting with with the tissues in the body [3]. The attenuation of the x-ray beam along a given ray path is determined by the sum over all tissues along that ray path of the product of length of the ray path through each tissue and the effective linear attenuation coefficient, μ, of that tissue average over the x-ray spectrum.

In modern CT, attenuation profiles are typically acquired a 1000 times per 360 degrees rotation of the gantry [2]. The sinogram is a way of showing the raw acquisition data as a function of gantry angle in 2-D matrix [1]. Intuitively, to invert this process and recover an image from its sinogram, it is natural to attempt what is known as back-projection. Mathematically, the back-projection can be shown as,

$$R^{'}[g](x_1, x_2) = \int_0^{2\pi} g(\theta, x_1 cos\theta + x_2 sin\theta) d\theta \tag{1}$$

The notation $R^{'}$ is used for the back-projection to emphasize that it is different from the inverse Radon transform.

2.2 The Fourier Slice Theorem

The Fourier Slice Theorem gives a simple relation between the 2-D Fourier transform $\hat{f}$ of an image f and the 1-D Fourier transform $\hat{g}(\theta, \omega)$ of the data $g(\theta, s)$ with respect to the s variable, where $g = R[f]$.

The Fourier Slice Theorem states,

$$\widehat{R[f]}(\theta, \omega) = \sqrt{2\pi} \hat{f}(\omega\theta), \tag{2}$$

in which the 1-D Fourier transform of the data *R[f]* with respect to the s variable at a fixed θ is equal to the 2-D Fourier transform of the image restricted to the corresponding line with direction vector θ scaled by $\sqrt{2\pi}$ [1]. One can then apply the inverse 2-D Fourier transform to recover the original image. This process is called *Fourier Reconstruction*.

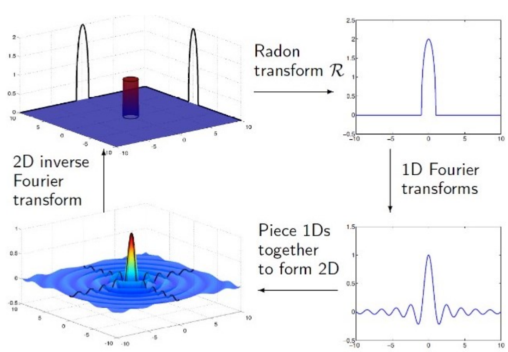

Fig 1 Specification of the Fourier reconstruction method. Each projection undergoes a 1-D transform, and then all the Fourier transforms are pieced together to show the Fourier transform of the image. An inverse 2-D transform then produces the image [1].

2.3 Filtered Back-projection

Filtered back-projection is an analytic reconstruction algorithm designed to overcome the limitations of conventional back-projection [4]. Derivation of the FBP will be omitted for now with the final solution being presented below,

$$\frac{1}{4\pi}\int_0^{2\pi}\Lambda[g](\theta, x_1 cos\theta + x_2 sin\theta)d\theta \tag{3}$$

where Λ denotes the filtering operator,

$$\Lambda[g](\theta, s) = \frac{1}{\sqrt{2\pi}}\int_{-\infty}^{\infty}\hat{g}(\theta,\omega)e^{i\omega s}|\omega|d\omega. \tag{4}$$

The variable $|\omega|$ represents the ramp filter. In order to account for the discrete projection data the values of $|\omega|$ are made discrete rather than continuous. An important part of the FBP algorithm is the ramp filter. The ramp filter accounts for the under sampling of high frequency signals which in turn blurs the image in the spatial domain. However, this can pose a problem in some cases. Although the ramp filter is a vital component, it is a high-pass filter. This means that high frequency noise will be amplified if present, leading to a noisy/grainy reconstruction. Therefore, additional filtering is necessary in the form of a low pass filter $\Psi_{LP}(\omega)$ which is multiplied by $|\omega|$ in the frequency domain [1].

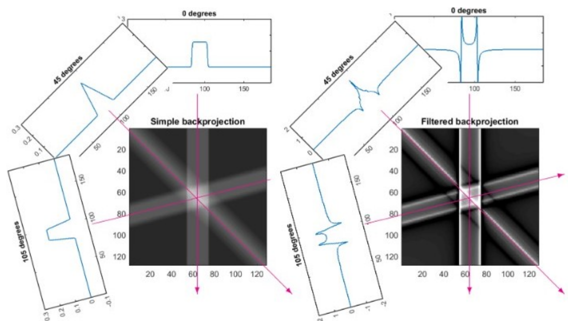

Fig 2 Simple illustration of the FBP algorithm for the case of three projections [1].

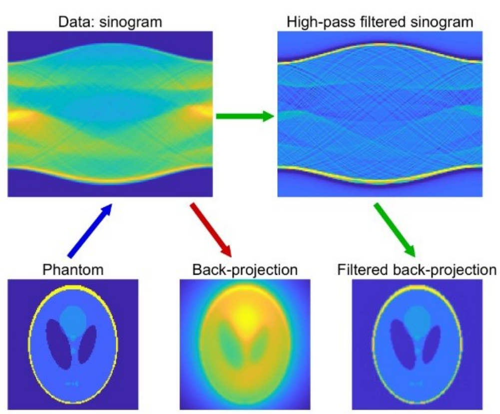

Fig 3 Illustration of the ramp filter in the FBP algorithm on a sinogram and the reconstruction of the Shepp-Logan Head Phantom [1].

2.4 *Iterative Reconstruction Method*

The iterative reconstruction (IR) method is an alternative process to FBP reconstruction. The area where iterative reconstruction is currently being utilized the most is in PET (Positron Emission Tomography) and SPECT (Single Photon Emission Computed Tomography) [9]. Compared to the FBP reconstruction method IR has an improved distribution of data. A "simple explanation" of the iterative reconstruction method can be seen below in Figure 4.

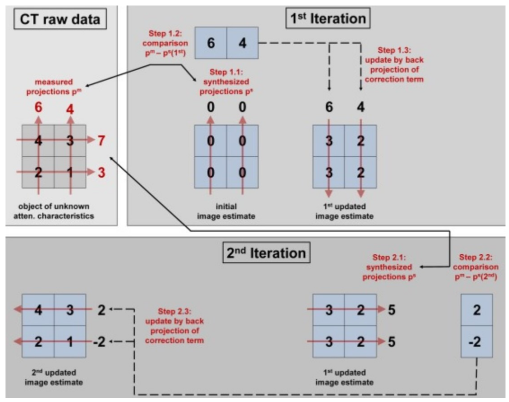

Fig 4 Simplified example of the iterative reconstruction cycle for a 2x2 matrix consisting of two unknown coefficients and a corresponding image matrix of 2x2 pixels [9].

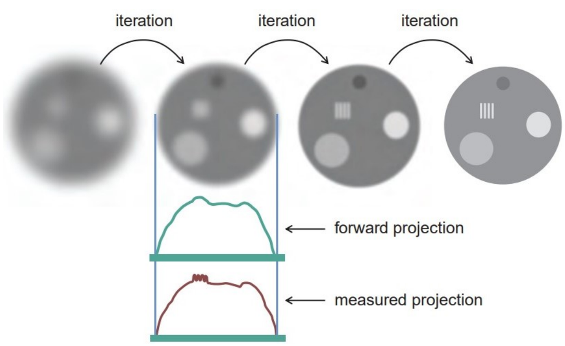

Fig 5 The logic behind iterative CT image reconstruction [3].

Iterative reconstruction techniques go through a series of iterations in the process of CT reconstruction. The first image may start as a guess, a constant image, or as a filtered back-projection image. The iteration process then goes through series of updates (iterations), which drive the CT image toward a final, accurate depiction of the object that was scanned [3]. Most iterative algorithms use similar fundamental logic-the current estimate of the image is used to generate forward projections, which are then compared to the actual measured projections as shown is Figure 5 [3]. The difference between the forward projection and measured projection is the error matrix, which is computed for all projections around 360 degrees. Each specific iterative algorithm uses the error matrix to update the next iteration of the image, with the intent of reducing the error matrix in the subsequent iteration.

A mathematical depiction of IR can be seen as,

$$R \cdot f = p, \tag{5}$$

where R is the radon transform of the image and NxM matrix. The variable f is the image to be reconstructed and a Nx1 matrix and p is the measured projection. Further breakdown of equation 5 leads to,

$$f_{\nu+1} = f_\nu + r_n(p_n - r_n \cdot f_\nu) \tag{6}$$

with ν representing the ν_{th} iteration.

3 Methodology and Results

3.1 Filtered Back-projection Algorithm

3.1.1 Sinogram

The first step to performing FBP is obtaining the sinogram of the image of interest. Using python, a function was made that would rotate the image by an array of angles and take the projections. However, another function was called before hand that would pad the image with zeros such that the new image is a square with sides equal to the diagonal of the original in size. Padding the image beforehand rather than allow the rotate method to expand the image because the image expands to different sizes depending on the angle of rotation. Every rotated image needed to be expanded to the same size so the collection of contributions can be stored within the same vector. Thus, the input variables would be the image of interest and the angles over which to compute projections.

The image used to test the sinogram function was a Shepp-Logan head phantom. The Shepp-Logan head phantom is a standard test image created by Larry Shepp and Benjamin F. Logan. It serves as the model of a human head in the development and testing of image reconstructio algorithms [3]. The projections were taken every 1°over a span of 360°. After verifying that the function provided the correct sinogram of the Shepp-Logan head phantom, to further evaluate the function I decided to use the image of cat next. I mean who doesn't like cats! The projections were sampled using the same process as the Shepp-Logan head phantom.

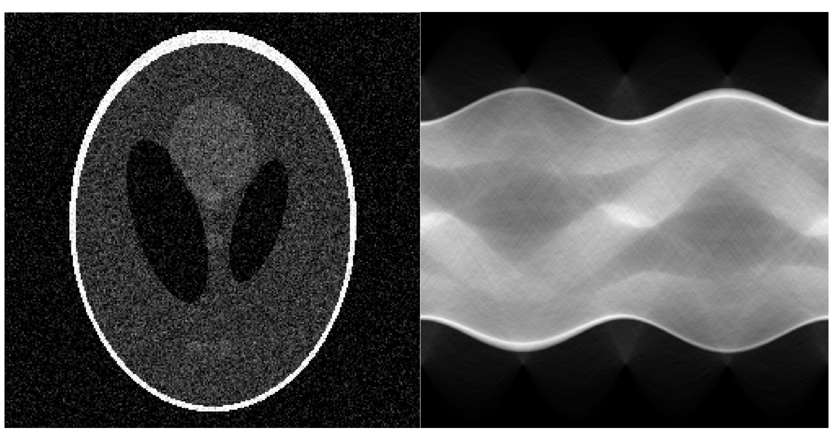

(a) (b)

Fig 6 (a) Image of Shepp-Logan head phantom and associated (b) sinogram.

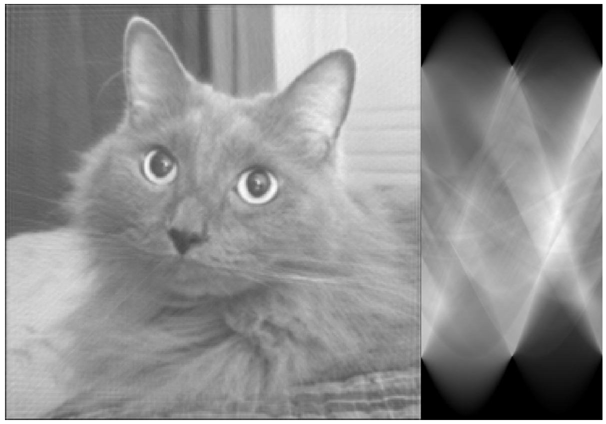

(a) (b)

Fig 7 (a) Image of cat and associated (b) sinogram.

3.1.2 Ramp Filter and Fourier Transform

As mentioned in the physics section, the simple back-projection operation produces a blurred version of the desired image. The desired image can be obtained by filtering the back projection with a ramp filter. The ramp filter was constructed as a column vector of the same length of the projections. The values fell within the interval of negative one and positive 1, with the absolute value taken right after.

Now with the ramp filter being complete, next came the step of taking the 1-D Fourier transform sinogram data. Initially, each contribution to the cat image 2-D Fourier transform began as all zeros. Each the 1-D Fourier transform was taken for each projection and then placed at the center of the next image contribution. The ramp filter would then be multiplied to each projection element in the (Fourier) domain. Each image contribution was rotated at the correct angle on the 2-D Fourier-space image and then added to the running representation of the image in Fourier space. Fig 8 shows the cat image in Fourier space.

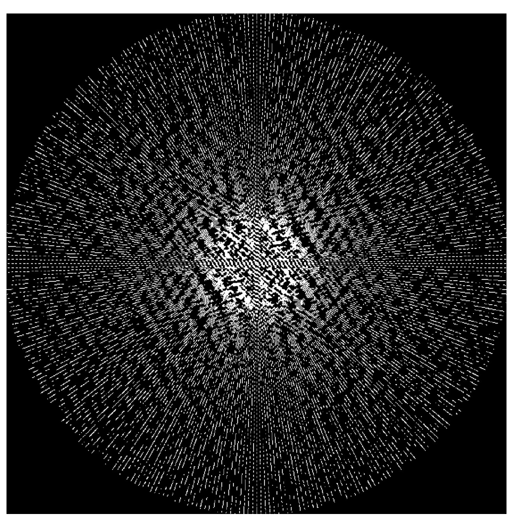

Fig 8 Photo of the cat image in the Fourier (frequency) domain.

3.1.3 Inverse Fourier Transform and Reconstructed Image

The final step was to take the inverse Fourier transform of the image to go from the Fourier domain back to the spatial domain. The resulting image however consisted of complex numbers, so only the real part of the image needed to be extracted. Fig 9 shows the resultant reconstructed image.

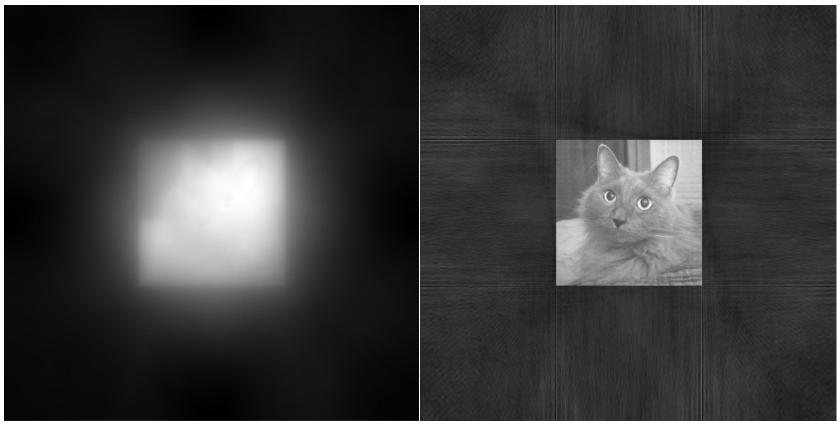

(a) (b)

Fig 9 (a) Image of reconstructed image without the ramp filter and (b) image of reconstructed image with the ramp filter.

Evaluation of the reconstructed image compared to the original was done using the ”eye test.” Fig 10 shows the original image and reconstructed image side by side. Although this method does not provide any quantitative analysis of the two images it does prove that the reconstruction algorithm was a success to some degree.

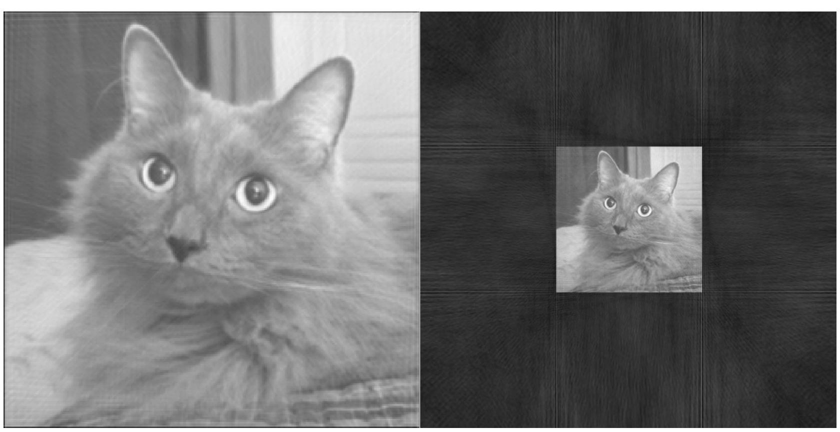

(a) (b)

Fig 10 (a) Image of cat and (b) reconstructed image from sinogram of the cat.

3.2 Iterative Reconstruction

The problem of image reconstruction from projections can be considered as a system of linear equations of the form seen in equation 5. In this case R will be used as the system matrix, and f and

p remain the same. The system matrix R has 12x9 elements, and p has 12x1 elements. Therefore, the image, f, will have 9x1 elements. The elements of the system matrix give the proportion of the individual ray passing through the pixel, with each row in R representing a different ray passing passing through the pixels, producing a projection data in f.

Solving the system of linear equations can be done using numerous methods, however there was a way to calculate residual error alongside performing the image reconstruction. Two loops were used in the reconstruction algorithm. The first loop looped over a certain number of iterations, in this case 50. The second loop looped over each of the rays of the projection matrix. Within this loop the projection data for each row in the system matrix, and correction factor based on the difference between the actual and projected data were calculated. Using the correction factor updates could be made to image using each row of the system matrix.

A initial 3x3 test image was constructed of random values, and reshaped into a 9x1 matrix so the matrix arithmetic would work. The test image was run through the algorithm and the residual error was plotted and can be seen in Fig 12.

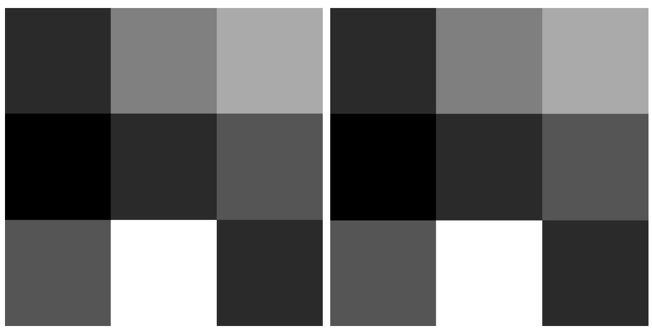

(a) (b)

Fig 11 (a) Test image and (b) reconstructed image.

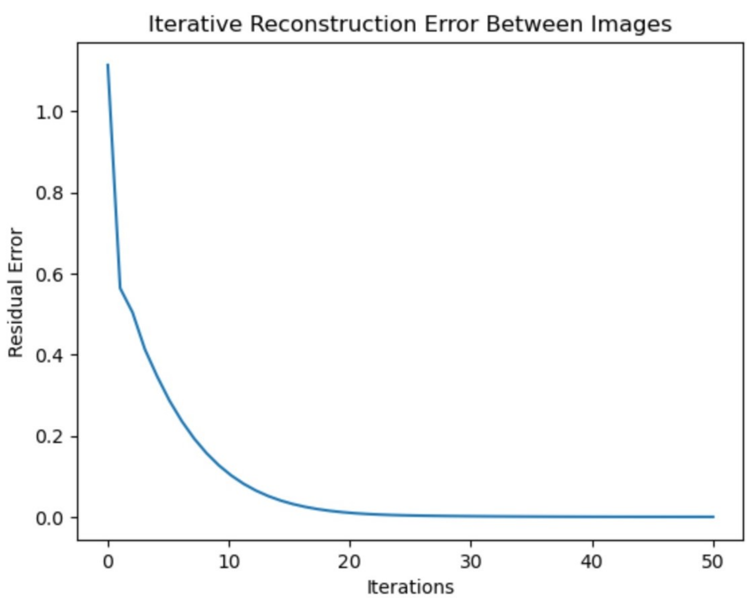

Fig 12 Plot of the residual error as a function of the number of iterations for the test image.

Fig 11 shows the original test image and the reconstructed image. Using the ”eye test” we can assume that the algorithm works to a certain extent. But when combined with the results of Fig 12 one can surmise the reconstruction algorithm works exceptionally well especially over a great number of iterations.

3.2.1 Alteration of System Matrix

The elements of the system matrix were altered and the effects on the reconstructed image were observed. All nonzero elements of the system matrix were changed to 1. The test image was put through the algorithm and although the reconstructed image ”looked” the same the residual error was quite different. Fig 13 shows the reconstructed image using the altered system matrix and the reconstructed image using the original system matrix. Fig 14 shows the difference in both cases the residual error calculated as the number of iterations increases.

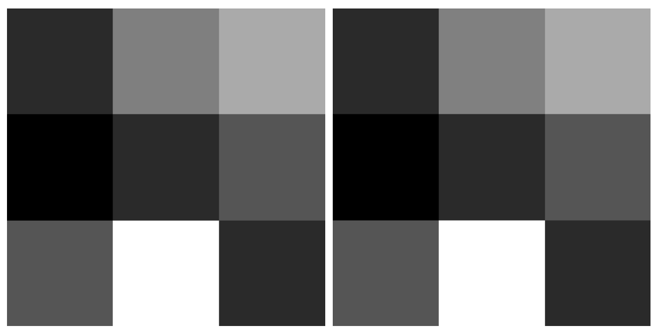

(a) (b)

Fig 13 (a) Reconstructed image using the original system matrix and (b) reconstructed image using the altered system matrix.

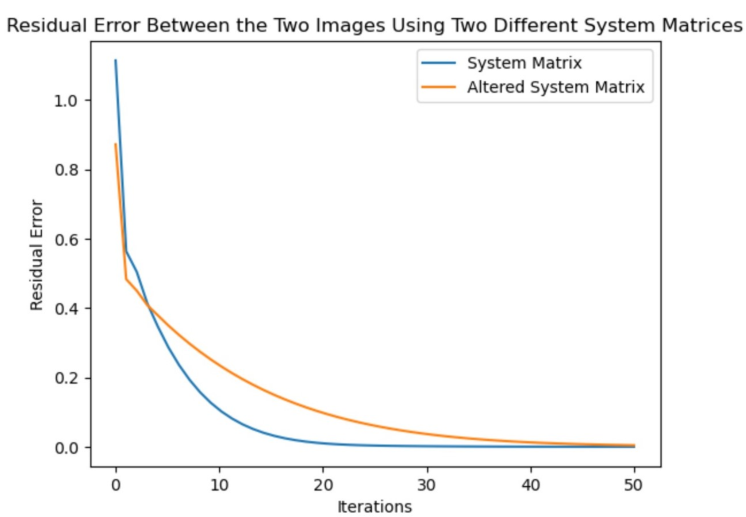

Fig 14 Plot of the residual error depending on the system matrix used.

From Fig 14 one can see that the error between the reconstructed image and the original weighs heavily on the system matrix. This only emphasizes the importance of having the appropriate values associated with each element (pixel). In terms of CT data acquisition these values would represent the attenuation coefficients of the various mediums that interact with the traversing ray.

4 Summary and Conclusion

The algorithms constructed have yielded adequate results. The filter back-projection algorithm produces an eye pleasing reconstructed image of the sinogram data. There were a few assumption made to ensure that the algorithm ran optimally; (1) rays travel in straight lines, (2) ray intensity attenuates exponentially, and (3) the sinogram represents a perfect representation of the object being imaged. However, unlike the iterative reconstruction algorithm there was no system implemented to examine the precision of the reconstructed image.

It would also be insufficient using the IR technique to attempt to reconstruct the image of the cat. For one, the system of equations we have to solve is large. Each sampling of the Radon transform produces an equation in the system while each pixel corresponds to an unknown, the color value for that pixel. If the system of equations is over-determined, with more equations than unknowns, then the system does not have an exact solution. If the system is under-determined, with more unknowns than equations, then there may be infinitely many solutions, with only one of which being the correct solution. But the IR technique would ultimately reconstruct the image in a much shorter time than the FBP technique.

The IR algorithm was able to reconstruct the image precisely in only a few iterations. The greater the number of iterations the better the quality and validity of the reconstructed image. It wasn't until the system matrix was altered that the number of iterations needed to be large enough to effectively reconstruct the image.

In terms of a clinical setting radiologist have "grown up" looking at FBP images often feel more comfortable reviewing these images rather than IR ones even as the concern for patient radiation dose has driven the acceptable signal-to-noise ratio progressively lower and lower.

Acknowledgments

I would like to thank Dr. Wise for a wonderful course in which I learned a great amount and was able to complete this project. This has helped become a more proficient computer programmer and allowed me to take on task relevant to the medical physics field.

References

1. Hansen, P. C., Jorgensen, J., amp; Lionheart, W. R. B. (Eds.). (2021). *Chapter 6: Filtered back-projection - fundamentals of algorithms*. Society for Industrial and Applied Mathematics. Retrieved March 2, 2023, from https://epubs.siam.org/doi/10.1137/1.9781611976670.ch6

2. Pontana, F., Hounsfield, G. N., Prakash, P., Kim, Y., amp; Baumueller, S. (2019, April 16). *Image reconstruction: Part 1 – understanding filtered back projection, noise and image acquisition*. Journal of Cardiovascular Computed Tomography. Retrieved February 26, 2023, from https://www.sciencedirect.com/science/article/pii/S1934592519300607

3. Bushberg, J. T., Seibert, J. A., Leidholdt Jr., E. M., amp; Boone, J. M. (2012). *The Essential Physics of Medical Imaging*. Wolters Kluwer / Lippincott Williams amp; Wilkins.

4. Bell, D. J. (2020, April 19). *Filtered back projection: Radiology reference article*. Radiopaedia Blog RSS. Retrieved March 3, 2023, from https://radiopaedia.org/articles/filtered-back-projection-1

5. Gajera, J. (2021, February 24). *Iterative Reconstruction (CT): Radiology reference article*. Radiopaedia Blog RSS. Retrieved March 3, 2023, from https://radiopaedia.org/articles/iterative-reconstruction-ct?lang=us

6. Zeng, G. L. (2014, October 30). *Revisit of the ramp filter*. IEEE transactions on nuclear science. Retrieved March 4, 2023, from https://www.ncbi.nlm.nih.gov/pmc/articles/PMC4341983/

7. Virginia Commonwealth University. (n.d.). *Iterative Reconstruction*. Retrieved March 4, 2023, from https://people.vcu.edu/ mhcrosthwait/clrs322/Iterativereconstruction.htmlIR1

8. Rice University. (n.d.). *Filtered Back Projection*. Retrieved March 3, 2023, from https://www.owlnet.rice.edu/ elec539/Projects97/cult/node2.html

9. Stiller, W. (2018, October 26). *Basics of iterative Reconstruction Methods in Computed Tomography: A vendor-independent overview*. European Journal of Radiology. Retrieved March 4, 2023, from https://www.sciencedirect.com/science/article/pii/S0720048X18303747?via

10. Flores, L., Vidal, V., amp; Verdú, G. (2015, November 17). System matrix analysis for computed tomography imaging. PLOS ONE. Retrieved April 25, 2023, from https://journals.plos.org/plosone/article?id=10.1371

Biographies and photographs of the other authors are not available.

List of Figures